Research

New Phytologist

Multiple time scale optimization explains functional trait responses to leaf water potential

Aidan Matthews[1], Gabriel Katul[2] and Amilcare Porporato[1]

[1]Department of Civil and Environmental Engineering and High Meadows Environmental Institute, Princeton University, Princeton, NJ 08540, USA; [2]Department of Civil and Environmental Engineering, Duke University, Durham, NC 27708, USA

Author for correspondence:
Amilcare Porporato
Email: aporpora@princeton.edu

Received: *28 January 2024*
Accepted: *22 July 2024*

New Phytologist (2024) **244:** 426–435
doi: 10.1111/nph.20035

Key words: carbon assimilation, optimization, plant hydraulics, stomatal control, trait coordination, vulnerability curve, xylem.

Summary

- Plant response to water stress involves multiple timescales. In the short term, stomatal adjustments optimize some fitness function commonly related to carbon uptake, while in the long term, traits including xylem resilience are adjusted. These optimizations are usually considered independently, the former involving stomatal aperture and the latter carbon allocation. However, short- and long-term adjustments are interdependent, as 'optimal' in the short term depends on traits set in the longer term.
- An economics framework is used to optimize long-term traits that impact short-term stomatal behavior. Two traits analyzed here are the resilience of xylem and the resilience of nonstomatal limitations (NSLs) to photosynthesis at low-water potentials.
- Results show that optimality requires xylem resilience to increase with climatic aridity. Results also suggest that the point at which xylem reach 50% conductance and the point at which NSLs reach 50% capacity are constrained to approximately a 2 : 1 linear ratio; however, this awaits further experimental verification.
- The model demonstrates how trait coordination arises mathematically, and it can be extended to many other traits that cross timescales. With further verification, these results could be used in plant modelling when information on plant traits is limited.

Introduction

An ongoing challenge in global climate and integrated land surface models is to broadly connect stomatal conductance to plant hydraulics and mathematically close the soil–plant-atmosphere system. This mathematical closure entails a connection between root zone and leaf water potential that is impacting stomatal regulation (Katul *et al.*, 2012; Buckley, 2017). This is a particular concern in conditions of water stress and over longer time scales (Katul *et al.*, 2012; Buckley, 2017). At the individual plant scale, plant water-use strategies determine the adaptive relation between plants and their environment. These relations involve a myriad of plant traits and multiple temporal scales ranging from 'instantaneous' to lifetime and generational. A distinction between 'trait-syndrome' and 'response based' metrics for quantifying water-use strategies has been offered to highlight the significance of these scales and their separation (Kannenberg *et al.*, 2022). The former encompasses measurable plant traits that change over weeks, seasons, or even generations, while the latter is concerned with stomatal closure changes with time and short-term environmental variables (e.g. sub-hourly). Such metrics are linked because long-term plant traits set the conditions that determine short-term responses and vice versa. This work aims to demonstrate how plant trait optimization hypotheses traditionally limited to either long-term traits (e.g. carbon economy) or short-term responses (e.g. stomatal dynamics) can be coupled to find optimal solutions to traits that affect both simultaneously.

To incorporate both, a modeling system is used that includes carbon and water dynamics. Plant water-use strategies and carbon uptake are intertwined (Nikinmaa *et al.*, 2013; Diaz-Espejo & Hernandez-Santana, 2017; Holttä *et al.*, 2017; Potkay & Feng, 2022) through stomatal gas diffusion, coupled xylem–phloem water potentials, and carbon allocation to optimize hydraulics (Ehleringer & Cowan, 1986; Diaz-Espejo & Hernandez-Santana, 2017; Holttä *et al.*, 2017). Plant water potential, the resulting outcome of soil water availability and atmospheric demand, dictates flow in both the xylem and phloem hydraulic systems within a plant (Diaz-Espejo & Hernandez-Santana, 2017; Konrad *et al.*, 2019). Water potential directly limits photosynthesis through nonstomatal limitations (NSLs) (Vico & Porporato, 2008; Volpe *et al.*, 2011; Zhou *et al.*, 2013; Dewar *et al.*, 2018; Flexas *et al.*, 2018; Qiu & Katul, 2020). NSLs may be caused by mesophyll conductance, translocation in the phloem, maximum electron transport and carboxylation capacity, or cell turgor that can all limit photosynthesis at low-water potentials (Flexas *et al.*, 2008; Zhou *et al.*, 2013; Holttä *et al.*, 2017; Dewar *et al.*, 2018). Hence, capturing the plant-economics picture requires simultaneous consideration of the hydraulic and photosynthetic systems (Bloom *et al.*, 1985; Buckley *et al.*, 2017).

Modeling plant systems and plant traits requires consideration of the timescales over which traits change. The adjustment time of a trait is proportional to the energy investment (Ehleringer & Cowan, 1986). At the finest time scale, opening a stoma requires only an osmotic adjustment in two guard cells, and thus occurs in minutes. On the other hand, allocating carbon to grow branches or roots takes more energy and occurs gradually over years (Ehleringer & Cowan, 1986; Vico *et al.*, 2011). If plants behave optimally due to evolutionary selection, then the question remains of how plants manage optimizations on different time horizons. In classical microeconomics, it is typical to consider a 'short run' where some costs such as the technology used and the land are fixed, while other costs, like labor, are variable. In the 'long run,' all costs are considered variable, with the fixed costs being changed within the cost functions of the day to day optimization (Binger & Hoffman, 1998). Similarly, the adjustments made by stomata and water potential are orders of magnitude faster than the rate at which other traits change; and in fact, the difference in rates is so large that in models of stomatal behavior, these traits are considered quasi-stationary (Damour *et al.*, 2010; Wang *et al.*, 2020).

Here, long run is defined as any trait adjustment that occurs at a significantly slower rate than the rate of stomatal action. This includes traits that may change over weeks to those that remain near constant throughout the life of the plant, and only change over generations. The cost associated with investing in long-run traits comes directly from the energy or carbon associated with investment or from an indirect loss of potential carbon gains from inhibiting plant productivity in another way. According to the generally accepted notion of evolutionary trade-offs, some cost *must* exist for improving one trait or else the improvement would have already been made in the course of evolution (Roff & Fairbairn, 2007).

The inseparability of long- and short-term traits can be seen in plant hydraulics. For example, the relation between stomatal conductance and leaf water potential depends on xylem resistance to low-water potentials, thus influencing optimal short-term behavior (Sperry *et al.*, 2016). Conversely, short-term optimization dynamics, for instance, the degree of isohydry (maintenance of a certain leaf water potential) influences the degree of xylem resilience that is optimal. While xylem resilience is developed over long time spans, the water potential adjusts approximately instantaneously on the same time scales as stomatal adjustments (Wolf *et al.*, 2016; Wang *et al.*, 2020). Because of these complications, traits at the intersection of long- and short-term dynamics thus far have not been modeled using optimization hypotheses.

In this paper, short- and long-term dynamics are combined by framing the plant as a 'business' that must optimize over two time horizons. We assume that water status changes near instantaneously in response to meteorological and stomatal activity – this is the short-run response (Wolf *et al.*, 2016; Wang *et al.*, 2020). The optimal strategy of these instantaneous adjustments depends on the resilience of different plant traits or processes to water potential, ψ (Wolf *et al.*, 2016; Sperry *et al.*, 2017; Mrad *et al.*, 2019). Specifically, we focus on hydraulic conductance, the ease with which liquid water can flow through the plant hydraulic network and its reduction with water potential (ψ) due to embolism (Tyree & Sperry, 1988; Hacke *et al.*, 2004; Sperry & Hacke, 2004; Zimmermann, 2013; Mrad *et al.*, 2018; Johnson *et al.*, 2022), as well as low-water potential effects on NSLs (Vico & Porporato, 2008; Dewar *et al.*, 2018). These traits have so far not yet been modeled using an optimization framework due to their complex interactions with short-term water potential fluctuations, which is dealt with here by using a dual time horizon model.

Description

Hydraulic and photosynthetic limitations

Plant hydraulics provide physical boundaries on stomatal operation (Van den Honert, 1948; Bonner, 1959; Brodribb *et al.*, 2017). For negligible plant capacitance, mass conservation necessitates that the demand for water due to atmospheric aridity is met by the supply of water stored in soil pores (Sperry *et al.*, 2016). Demand for water or evaporation (E) is determined by the difference in humidity inside the leaf, q_i, and in the atmosphere, q_a. Diffusion occurs proportionally to stomatal conductance, g_s (mol m^{-2} s^{-1}) so that:

$$E = g_{sa}\left(q_i(\psi_l) - q_a\right) \approx g_s D \qquad \text{Eqn 1}$$

where D (kg kg^{-1}) is the constant specific humidity deficit in the atmosphere (Table 1). For simplicity, the role of aerodynamic conductance is ignored. It is further assumed that the relative humidity in the sub-stomatal cavity is nearly 100%. These assumptions, while appearing restrictive, do not qualitatively affect the results.

On the supply side, the liquid water flow through the plant Φ is approximated as (Manzoni *et al.*, 2014; Porporato & Yin, 2022):

$$\Phi = K(\psi_l)\left|\psi_l - \psi_s\right| \qquad \text{Eqn 2}$$

where ψ_s and ψ_l are the soil and leaf water potentials and $K(\psi)$ is the conductance (mol m^{-2} s^{-1} MPa^{-1}).

The $K(\psi)$ is modeled as a single vulnerability curve (Tyree & Sperry, 1988):

$$K(\psi_l) = \frac{K_{max}}{1 + \exp\left(-k_K\left(|\psi_l| - |\psi_{50K}|\right)\right)} \qquad \text{Eqn 3}$$

where k_K and $|\psi_{50K}|$ are considered fixed in the short-run optimization. The choice of ψ_l as the restrictive water potential is justified by the hydraulic segmentation hypothesis (Zimmermann, 2013; Johnson, 2014; Konrad *et al.*, 2019; Johnson *et al.*, 2022), whereby $K(\psi_l)$ is the most restrictive conductance in the plant hydraulic network. In the case when root or another hydraulic conductance is limiting, the intermediate water potentials leading to this limitation are still dependent on ψ_l. Thus, the use of ψ_l can lead to effectively the same results as a distributed model. Use of more detailed representations that account for the distributed nature of the resistance to flow from soil to roots to leaves is

Table 1 A list of symbols used and their meaning.

Variable	Description	Unit
E	Evaporation from the leaf	mol m^{-2} s^{-1}
Φ	Liquid water flux through the plant	mol m^{-2} s^{-1}
s	Relative soil moisture	–
D	Specific humidity deficit	kg kg^{-1}
g_s	Stomatal conductance	mol m^{-2} s^{-1}
g_{crit}	Maximum g_s allowed by plant hydraulics	mol m^{-2} s^{-1}
g_s^*	Optimal g_s which maximizes photosynthesis	mol m^{-2} s^{-1}
ψ_l	Leaf water potential	MPa
ψ_l^*	Optimal ψ_l which maximizes photosynthesis	MPa
ψ_s	Soil water potential	MPa
K_{max}	Maximum water conductance through the plant	mol m^{-2} s^{-1} MPa^{-1}
$f_K(\psi_l)$	Conductance vulnerability curve	–
k_K	Maximum slope of the conductance vulnerability curve	–
ψ_{50K}	ψ_l at which 50% of conductance is lost	MPa
A	Net photosynthesis accounting for NSLs	mol m^{-2} s^{-1}
A_0	Photosynthesis not accounting for NSLs	mol m^{-2} s^{-1}
c_i	Carbon dioxide concentration inside the stomatal cavity	mol mol^{-1}
c_a	Atmospheric carbon dioxide concentration	mol mol^{-1}
$f_l(\psi_l)$	Photosynthesis vulnerability curve from NSLs	–
k_L	Maximum slope of the NSL vulnerability curve	–
ψ_{50L}	ψ_l at which 50% of photosynthetic capacity is reached	MPa
Θ	The carbon cost of investment in long-term traits	mol s^{-1}
α_k	The unit carbon cost of increasing $\lvert\psi_{50K}\rvert$ by 1 MPa	mol s^{-1} MPa^{-1}
α_L	The unit carbon cost of increasing $\lvert\psi_{50L}\rvert$ by 1 MPa	mol s^{-1} MPa^{-1}

possible (Manoli *et al.*, 2017) but make the analysis more complicated and do not change qualitatively the conclusions as Φ depends directly on leaf water potential (Sperry *et al.*, 2016).

By equating the supply in Eqn 2 to the demand in Eqn 1, a relation between g_s and ψ_l can be derived as:

$$g_s D = K_{max} f_K(\psi_l)(\psi_s - \psi_l) \quad \text{Eqn 4}$$

For a constant D, when stomata open and g_s increases, the decreasing ψ_l creates a stronger pulling force but cavitation spread in the xylem also increases the resistance to flow. Eventually, a point is reached where any further stomatal opening is physically impossible because supply, inhibited by embolism and cavitation spread, is unable to match demand. This maximum stomatal conductance permitted by plant hydraulics at a given level of ψ_s and D, g_{crit}, is the maximum value reached in the 'Hydraulics' (Fig. 1) (Manzoni *et al.*, 2013a, 2014). If g_s is increased above g_{crit}, runaway embolism occurs, breaking the hydraulic continuity and preventing water flow to the leaves. For this reason, g_{crit} is a hydraulic upper bound in the stomatal optimization, which decreases with lower humidity (higher D) and drier soil (lower ψ_s). Note that if one uses a form of conductance continuously changing from roots to leaves (e.g. Sperry *et al.*, 2016), the relation between $-\psi_l$ and g_s would be monotonically increasing and thus no g_{crit} would be present (Johnson *et al.*, 2022).

The carbon dioxide supplied by the atmosphere through diffusion into the stomata is:

$$A = \frac{g_s}{1.6}(c_a - c_i) \quad \text{Eqn 5}$$

where c_a (mol m^{-2}) is atmospheric carbon concentration, assumed constant in the short-run optimization, and c_i is the concentration inside the stomata; the 1.6 factor accounts for the difference in molecular diffusion coefficient between CO_2 and H_2O. This supply is balanced by the biochemical demand for carbon dioxide that depends on the photosynthetic machinery. Since the biochemical demand is an increasing function of c_i and ψ_l (see Supporting Information Methods S1 for details on the used formulation), it can be expressed as:

$$A(c_i, \psi_l) = A_0(c_i) f_L(\psi_l) \quad \text{Eqn 6}$$

where $A_0(c_i)$ is the biochemical demand that does not include NSLs, that is there is no explicit dependence on ψ_l. The $A_0(c_i)$ is expressed as a saturation function of c_i as conventionally done in the Farquhar photosynthesis model (Farquhar *et al.*, 1980). The multiplicative function, $f_L(\psi_l)$ (e.g. Tuzet *et al.*, 2003; Daly *et al.*, 2004; Salvi *et al.*, 2021), expresses NSLs (Vico & Porporato, 2008), which are limitations to photosynthesis due to several processes related to water potential. Some are linked to parameters associated with the $A_0(c_i)$ expression such as carboxylation capacity and maximum electron transport, while others are linked to the mesophyll conductance declining with reduced ψ_l in the cell (Flexas *et al.*, 2008; Volpe *et al.*, 2011) or cell turgor reducing the gas diffusional space (Vico & Porporato, 2008; Dewar *et al.*, 2018). A number of NSLs have also been linked to the other main hydraulic system in plants responsible for sugar and water transport – the phloem. As ψ_l is reduced, the ability of the phloem to pull water from the xylem by osmosis becomes impaired and sugar transport through the phloem becomes a limiting factor (Thompson & Holbrook, 2003; Nikinmaa *et al.*, 2013; Sevanto, 2014; Jensen *et al.*, 2016; Nakad *et al.*, 2021, 2023). All these NSLs are related to ψ_l and can be modeled similar to $f_K(\psi_l)$ in Eqn 4 as:

$$f_L(\psi_l) = \frac{1}{1 + \exp\left(-k_L\left(|\psi_l| - |\psi_{50L}|\right)\right)} \quad \text{Eqn 7}$$

with parameters ψ_{L50} and maximum slope k_L considered fixed in the short-run optimization.

This equation can be seen in the 'NSL' plot (Fig. 1).

As stomata open, A increases because of increased carbon diffusion into the leaf (A_0 increases). Yet, because $|\psi_l|$ also increases, A is limited by the NSL through $f_L(\psi_l)$. This leads to A being a concave down function of both g_s and ψ_l ('Full Photosynthesis' Fig. 1). However, because many models of photosynthesis do not include

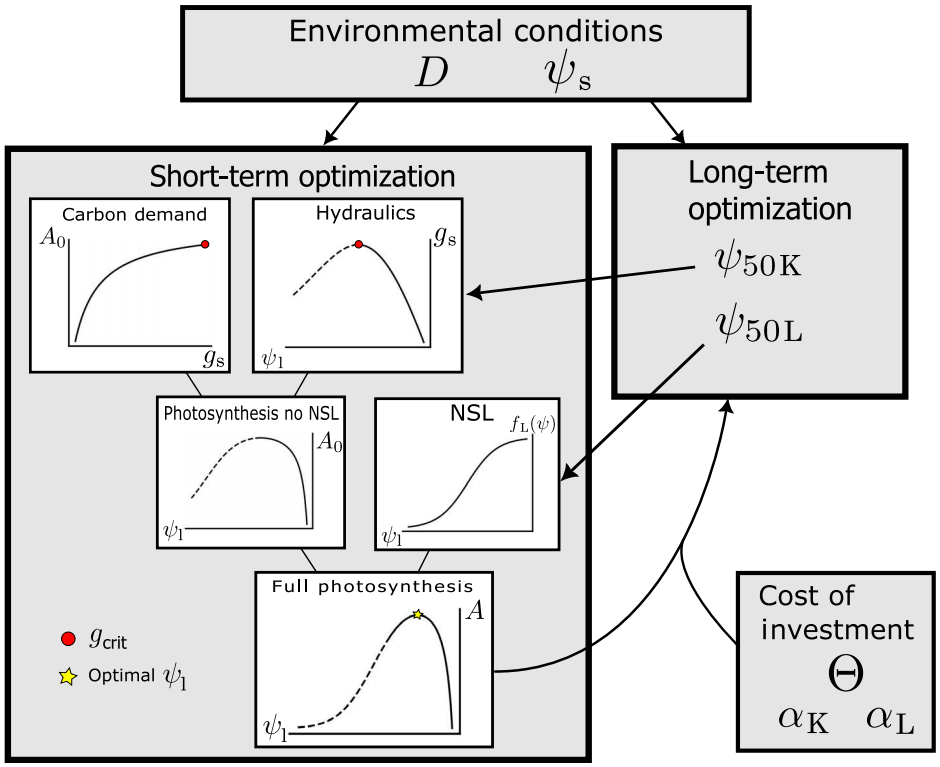

Fig. 1 A conceptual diagram showing the key relations between variables expressed in Eqns 4–7. The star in the 'Full Photosynthesis' plot is the short-term maximum A possible given environmental conditions and certain traits (ψ_{50K} and ψ_{50L}). The long-term optimal traits are determined to maximize the A that is achievable in the short term given the costs of investment in the traits (α_K and α_L). The dashed lines represent realms past which the equations still exist mathematically but would not feasibly be reached by plants due to excessive embolism. NSL refers to nonstomatal limitations on photosynthesis. D is specific humidity deficit, ψ_s is soil water potential, ψ_l is leaf water potential, g_s is stomatal conductance, A is photosynthesis, A_0 is photosynthesis not including NSLs, ψ_{50K} and ψ_{50L} are the water potentials at which conductance and photosynthesis are reduced to 50% capacity, $f_L(\psi_l)$ is the photosynthesis vulnerability curve from NSLs, α_K and α_L are the unit costs of increasing $|\psi_{50K}|$ and $|\psi_{50L}|$ by 1 MPa, respectively, and Θ is the total cost of investment of investing in long-term traits.

NSLs, this concavity has been overlooked in many past models (Wang *et al.*, 2020).

When NSLs are not included, maximum photosynthesis is achieved at maximum stomatal aperture determined only by plant hydraulics, g_{crit} (red dot Fig. 1). When NSLs are included, maximum photosynthesis is achieved at an optimal $|\psi_l^*|$ and g_s^* (yellow star Fig. 1) that is lower than $|\psi_{crit}|$ and g_{crit}. If plants maximize A, then there is a straightforward stomatal optimization model (SOM) that arises directly from hydraulics and photosynthesis without relying on additional cost or constraints (Dewar *et al.*, 2018). The SOM hypothesizes that plants should adjust g_s until ψ_l^* is reached to maximize A, and has been suggested previously using different forms of NSLs (Dewar *et al.*, 2018; Wang *et al.*, 2020). This is the short-term optimization that the proposed model assumes plants adhere to.

Note that conventional models known as 'diffusive conductance' or 'photosynthesis-stomatal conductance' models combine Eqns 5 and 6, but set $f_L(\psi_l) = 1$, and then complement these two equations by either an empirical expression linking g_s to A/c_a (Ball *et al.*, 1987; Leuning, 1995) or employ arguments that plants regulate g_s to maximize A for a given water loss per unit leaf area. The resulting parameters (e.g. the marginal water-use efficiency) are then reduced in an ad-hoc manner by ψ_l or soil moisture (Lai *et al.*, 2000; Tuzet *et al.*, 2003; Daly *et al.*, 2004; Manzoni *et al.*, 2011).

Optimization in the long run and trait coordination

Plant traits tend to be coordinated with one another (Chen *et al.*, 1993; Manzoni *et al.*, 2013b; Reich, 2014; Mencuccini *et al.*, 2015; Li *et al.*, 2021; Xu *et al.*, 2021). A long-term trait coordination is optimal when it allows for short-term optimizations to occur simultaneously. For instance, optimizing the risk of xylem embolism and cavitation spread would simultaneously optimize another aspect like maximizing photosynthesis. This type of coordination/optimization process is difficult to model due to the manifold interactions at different time scales: Adjusting long-term traits impacts short-term stomatal behavior, and short-term stomatal behavior determines the net impact of long-term trait adjustment.

In the short term, the degree of stomatal aperture is varied assuming constant plant traits such as xylem resistance to embolism or the parameters describing the $A_0(c_i)$. In the long term, most inputs (i.e. traits) are variable. A business may buy new technology, which then changes the conditions for short-term optimization. Analogously, plants may invest in long-term traits that in turn impact what stomatal behavior is optimal. If plants invest in resilience to water stress, then stomata can open more often and increase net carbon assimilation. Yet investing in resilience means not investing in other areas such as growth and reproduction (Mencuccini, 2003) or defenses (Novick *et al.*, 2012). While this analogy appears to give plants agency, it should be clarified that natural selection for optimal efficiency is what has led to the hypothesized optimal investment strategies in modern-day plants. The 'investments' in traits may be direct, in terms of devoting further carbon to strengthen xylem conduits, or indirect by through trade-offs with other less obvious aspects of plant fitness (Roff & Fairbairn, 2007).

Plant traits that influence short-term stomatal optimization dynamics are particularly important to improve models of

stomatal behavior that rely on knowledge of these traits. Analyzing the resilience of different plant processes to a decrease in water potential requires considering traits related to the response (vulnerability) curves to water potential. Other traits that can be analyzed are those associated with the photosynthetic machinery (e.g. $A_0(c_i)$) or phloem vascular properties (Jensen *et al.*, 2016) encoded in $f_L(\psi_l)$. While their effect on critical plant processes is evident, the physiological details of many of these vulnerability curves remain unclear (Dewar *et al.*, 2022; Lens *et al.*, 2022).

Here, the vulnerability curve captured by $f_K(\psi_l)$ (Eqn 3) and the NSL resilience to ψ_l captured by $f_L(\psi_l)$ (Eqn 7) are considered. In particular, the focus is on the water potential at which 50% of capacity is reached, ψ_{50K} and ψ_{50L}, while assuming a constant maximum slope of $k = 2$ for both (Salvi *et al.*, 2021). The slope, k, offers another dimension of potential optimization that can be addressed in future work.

Optimizing hydraulic vulnerability

To illustrate how a single trait can be optimized, the equation for short-term profit that only includes ψ_{50K} is considered. When doing so, complications arise because g_s (or ψ_l) appears in the equation as an unknown. To eliminate this short-term variation, we assume that in the short term, stomata maximize short-term profit for a constant ψ_{50K}. For the sake of notation later on, we will take ψ_l to be the control variable here because of its 1 : 1 relation with g_s, so that:

$$\psi_l^* = \underset{\psi_l}{\operatorname{argmax}}[A] \qquad \text{Eqn 8}$$

Thus $A(\psi_l^*)$ represents the maximum possible short-term profit, given constant environmental conditions and ψ_{50K} (gold star Fig. 1).

The gain from investing in ψ_{50K} is embedded within Eqn 3 that models xylem resilience to leaf water potential. As the xylem become more resilient to water stress ($-\psi_{50K}$ increases), the optimal stomatal behavior shifts to open more often under drier conditions and incurs lower costs from xylem embolism. Greater stomatal conductance allows for more assimilation and a greater total short-term profit for the plant.

We lump the costs for developing resilience (Lens *et al.*, 2022) into a single effective long-term cost, $\Theta = \alpha_k|\psi_{50K}|$, for simplicity assumed to be linear, with α (mol s^{-1} MPa^{-1}) representing the average cost per unit time that needs to be invested to increase resilience by 1 MPa. This yields a long-term optimization problem:

$$\max_{\psi_{50K}}\left[A\left(\psi_l^*, \psi_{50K}\right) - \Theta(\psi_{50K})\right] \qquad \text{Eqn 9}$$

occurring over a long-enough time that fluctuations in $A(\psi_l^*, \psi_{50K})$ from changing environmental conditions average out. Thus $A(\psi_l^*, \psi_{50K})$ represents the average short-term profit over the long term. Solving this optimization is done in two steps: calculating ψ_l^* by solving the short-term optimization problem for a given ψ_{50K} (Eqn 9), then iterating plausible values of ψ_{50K} (between 0 and −10 MPa) to obtain the long-term profit, $A - \Theta$.

The plot of long-term profit can be seen in Fig. 2 for different average soil water potentials, representing different mean climates. To the right of the maximums, the plant has not invested enough in hydraulic resilience and closes its stomata often to avoid xylem embolism, missing potential photosynthesis. To the left of the maximums, the plant has invested more carbon into resilience than it is gaining by allowing stomata to open more often. At the maximum:

$$\frac{\partial A}{\partial \psi_{50K}} = \frac{\partial \Theta}{\partial \psi_{50K}} = \alpha_K \qquad \text{Eqn 10}$$

This solution demonstrates that resilience should be invested in until the marginal gain ($\partial A/\partial\psi_{50K}$) is equal to the marginal cost, which in this case is a constant equal to the unit cost of resilience (α_K). Investing until marginal gain equals marginal cost is a core tenet of microeconomics and can be found in other plant optimizations, including SOMs (Bloom *et al.*, 1985; Binger & Hoffman, 1998; Wolf *et al.*, 2016).

Long-term optimization of nonstomatal limitations and hydraulic traits

Nonstomatal limitations on photosynthesis are minimally represented here by $f_L(\psi_l)$, see Eqn 7. Similar to the hydraulic case, we choose to optimize the leaf water potential at which photosynthetic capacity (A_0) reduces by 50%, ψ_{50L}, and maintain the slope constant ($k = 2$) (Salvi *et al.*, 2021). We assign α_L to be the carbon cost of increasing $|\psi_{50L}|$ by 1 MPa. Because NSLs depend on ψ_l, they are inextricably tied to plant hydraulics. Thus, ψ_{50L}

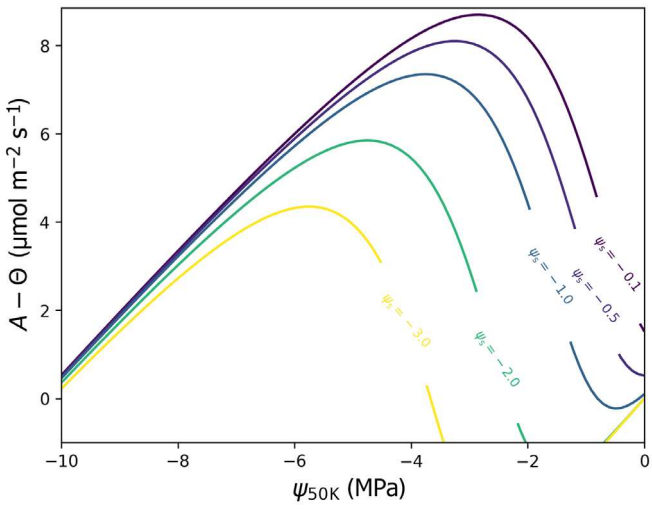

Fig. 2 A plot showing profit ($A - \Theta$) on the y-axis plotted against ψ_{50K} on the x-axis. Contours show different values of average soil water potential, ψ_s, in MPa. ψ_{50K} is the water potential at which conductance is reduced by 50%, A is photosynthesis, and Θ is the cost of investment in long-term traits (just ψ_{50K} here).

must be investigated with respect to ψ_{50K}. This co-limitation forms the basis for coordination.

The short-term optimization needs to be solved first for each pair of ψ_{50L} and ψ_{50K} to remove dependence on short-term variables. The short-term profit may be expressed as:

$$A(\psi_l^*, \psi_{50K}, \psi_{50L}) = \max_{g_s}[A(g_s(\psi_l), \psi_l, \psi_{50K}, \psi_{50L})] \quad \text{Eqn 11}$$

where no explicit θ is necessary because A includes the impact of NSLs. The long-term optimization that we hypothesize is:

$$\max_{\psi_{50K}, \psi_{50L}} [A(\psi_{50K}, \psi_{50L}) - \Theta(\psi_{50K}, \psi_{50L})] \quad \text{Eqn 12}$$

where

$$\Theta(\psi_{50K}, \psi_{50L}) = \alpha_K|\psi_{50K}| + \alpha_L|\psi_{50L}| \quad \text{Eqn 13}$$

To carry out this optimization, the first step, obtaining A as a function of only ψ_{50K} and ψ_{50L}, remains the same as before. The difference is that every combination of ψ_{50K} and ψ_{50L} needs to be optimized for. The second step, the long-run optimization, is more complicated with two variables. As before, we treat ψ_{50K} and ψ_{50L} as inputs that can be invested to increase output. We obtain level sets (or isoquants) where production is constant, that is $A(\psi_{50K}, \psi_{50L}) = A_x$ (Binger & Hoffman, 1998).

Results

Fig. 2 shows the results of the optimization of ψ_{50K} described in 'Optimizing hydraulic vulnerability' in the Description section, which keeps ψ_{50L} constant. Going from right ($\psi_s = -0.1$) to left ($\psi_s = -4.0$) (Fig. 2), the curves represent progressively drier climates and less mean water availability. The optimal ψ_{50K} for each ψ_s is the maximum value achieved in each contour. As visible, the optimal $|\psi_{50K}|$ increases with aridity because there is a greater gain from investing in resilience at low-soil moisture values; this is a repeatedly observed trend across rainfall gradients (Choat *et al.*, 2007; Li *et al.*, 2021). Also visible is a decreasing maximum long-term profit, as more water-limited systems incur higher investment costs and lower photosynthetic gains (from closing stomata). A lower long-term profit means that less free carbon/energy is available to be used for growth in drier environments. This agrees with the observation that plants in more arid environments are slower growing than those in wet environments.

The relation between ψ_s and optimal ψ_{50K} depends on several things including the details of the parameters selected for the photosynthetic model, fluctuating environmental conditions, and the cost of investment, α_K. This result is not compared to data as it is highly dependent on the choice of parameters, but could in theory be used to estimate the fitness cost of investing in resilience, α_k, by fitting to data.

The results of the long-term optimization of hydraulic and photosynthetic traits are presented in Fig. 3. The isoquants are shown as colored curves and illustrate combinations of inputs (ψ_{50K}, ψ_{50L}) that create that level of output. The fairly sharp corners mean that for a fixed ψ_{50K} no degree of increase in ψ_{50L} can increase total production, and vice versa. The dashed lines (Fig. 3) represent level sets of cost, that is $\Theta(\psi_{50K}, \psi_{50L}) = \alpha_K\psi_{50K} + \alpha_L\psi_{50L} = \Theta_x$. These lines are tangent to level curves if and only if that Θ_x is the minimum possible cost for a given level of production, A_x. Thus, we expect plants to operate at the points at which the isocost lines are tangent to the isoquants, which minimize cost for a given level of production (Bloom *et al.*, 1985). The optimal trajectory line represents the optimal trajectory of inputs if a plant were to change its level of output. The parameterization gives an optimal trajectory of about $\psi_{50L} \approx 0.5\psi_{50K}$ or $\psi_{50K} \approx 2\psi_{50L}$, that is a plant should invest so that its xylem are about twice as resilient to water stress than its photosynthetic apparatus.

The data (Fig. 3) come from an extensive literature survey (Manzoni, 2014). The data points include deciduous angiosperms, evergreen angiosperms and gymnosperms from boreal, temperate, dry tropical, and Mediterranean climates. The two data points at the bottom of the graph ($\psi_{50K} < -12$) are from Mediterranean climates. Due to the large variation in species and biome of origin, there is a large variety of strategies employed by various species. Different strategies including hydraulic redistribution, plant water storage, and deciduousness amongst others could change the optimal relation between ψ_{50K} and ψ_{50L} in unforeseen ways. Different data collection methods also add uncertainty. More data are needed to verify the results here and to identify the effects of different plant strategies on these derived relations.

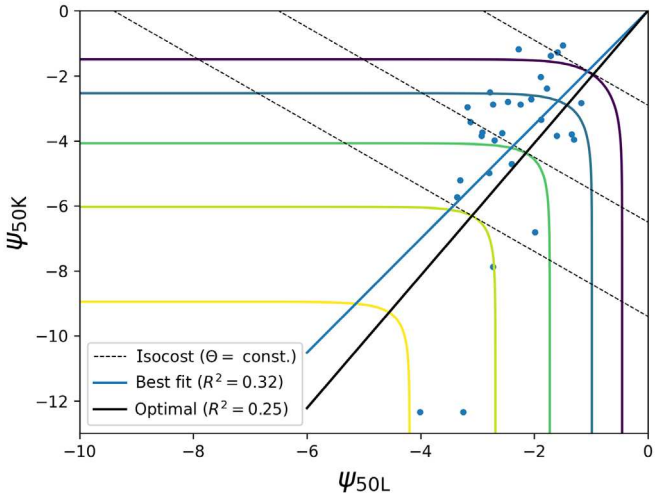

Fig. 3 A plot showing selected isocost and isoquant lines from different investments in ψ_{50K} and ψ_{50L} based on the model compared to data points from plants. The optimal trajectory passes through the tangent points of these lines. The isoquants, or level sets, of constant A (photosynthesis) values are curved. Dashed, straight lines are isocost lines representing constant values of Θ. The slope of the best fit line (solid blue) is 1.75 and the slope of the optimal trajectory line (solid black) is 2.04, a difference of 17%. ψ_{50K} and ψ_{50L} are the water potentials at which conductance and photosynthesis are reduced to 50% capacity, respectively. Data points are from the literature (Manzoni, 2014), originally from other studies for a variety of biomes and plants.

Nonetheless, the predictions offered here agree with this extensive dataset (Manzoni, 2014). The slope of the optimal trajectory can vary slightly for different parameterizations in the equation for photosynthesis (Methods S1), namely for K_{max}, D, and a_1 that represents a variety of photosynthetic parameters. Here, we chose the unit costs such that $\alpha_K = \alpha_L$ for simplicity. However, due to the relatively sharp corners of the isoquants, for αs of a similar order of magnitude, the tangent point will be near the corner of the isoquant. Thus, the optimal trajectory should not be sensitive to the precise numerical value of α. This is convenient because it is difficult to quantify the various αs, which encapsulate a myriad of physical traits (Choat *et al.*, 2007; Lens *et al.*, 2022).

While two specific traits (ψ_{50K} and ψ_{50L}) have been considered, this type of analysis can be extended to a suite of functional plant traits. For example, photosynthesis is given by the minimum of two limiting cases, Rubisco limitation by carboxylation capacity, $A_V \propto V_{cmax}$, or light/RuBP regeneration by maximum electron flux, $A_J \propto J_{max}$ (Farquhar *et al.*, 1980). Moreover, V_{cmax} and J_{max} are usually proportional to each other at a given reference temperature despite large variations in edaphic conditions (Leuning, 1997). It has been shown that both V_{cmax} and J_{max} decrease with water potential (Vico & Porporato, 2008; Zhou *et al.*, 2013, 2014). We define a water potential at which they decrease by half as ψ_{50V} and ψ_{50J}, respectively. If $\psi_{50V} \gg \psi_{50J}$, then under moderate water stress RuBP regeneration would always be limiting, while resources are invested in maintaining capacity for ψ_{50V}. This would be inefficient, so we can see from an intuitive argument that $\psi_{50V} \approx \psi_{50J}$ should be optimal.

Performing the entire optimization above, assuming a constant ψ_{50K} and varying ψ_{50V} and ψ_{50J} supports this argument. In Fig. 4, the limitation nature of the optimization creates a perfect right angle where $\psi_{50V} = \psi_{50J}$. As such, for any value of α_V or α_J, the optimal trajectory of values is just the line $\psi_{50J} = \psi_{50V}$. This finding agrees with published data (Zhou *et al.*, 2014). The data are from four species of the genus *Eucalyptus* across a climatic gradient in Australia, three species of the genus *Quercus* across a climatic gradient in Spain, and the species *Alnus glutinosa* and *Fraxinus excelsior* also from Spain (Zhou *et al.*, 2014). The data appears to agree with the optimal trajectory (a 1 : 1 line) with a coefficient of determination (R^2) value of 0.89.

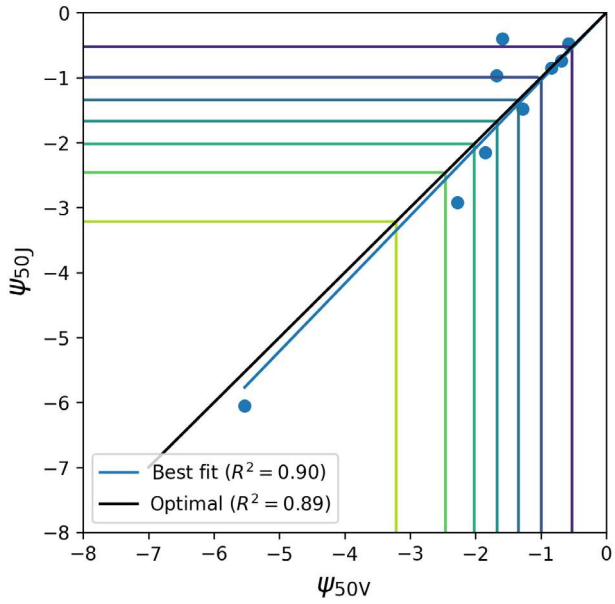

Fig. 4 A plot showing isoquants of different investments in ψ_{50V} and ψ_{50J} based on the model compared to data points from plants. The level sets (isoquants) of constant A (photosynthesis) are shown in color for different values of ψ_{50V} and ψ_{50J}. ψ_{50V} and ψ_{50J} are the water potentials at which carboxylation capacity and maximum electron transport are reduced to 50% capacity, respectively. The data is from an experimental study of NSLs and stomatal limitations (Zhou *et al.*, 2014).

Discussion

The proposed analysis captures with one main parameter, ψ_{50K}, the aggregate behavior of many interacting components and physical characteristics that determine hydraulic vulnerability. It encompasses the net result of different root, xylem, and leaf characteristics. Thus, investing in ψ_{50K} may take different forms and may even include root growth strategies. Similarly, ψ_{50L}, the resistance of photosynthetic capacity to water stress, encompasses the resistance of mesophyll, carboxylation capacity, phloem transport capacity and more (Holttä *et al.*, 2017; Dewar *et al.*, 2022). Because of these complications, it is nearly impossible to measure the carbon cost of investing (Θ) in these emergent traits. Fortunately, assuming a linear relation does not significantly change the link between ψ_{50K} and ψ_{50L}. This can be visually confirmed by the shape of the isoquants (Fig. 3). Because of the relatively sharp corners of the isoquants, any cost line that is a positive function of ψ_{50K} and ψ_{50L} will naturally be tangent to the lines near the corners, thus keeping the ratio between ψ_{50K} and ψ_{50L} within a small range.

To remove short-term fluctuations from the long-term optimization, the environmental conditions are held constant. Obviously, there are diurnal cycles and seasonal variations of most variables, especially photosynthetically active radiation, that influence stomatal dynamics. By focusing on periods of light saturating conditions, RuBisCo is limiting and not RuBP regeneration, and therefore, the linearization in Eqn S1.1 (Methods S1) is plausible. Once again, including the full nonlinearities in the biochemical demand can be carried out but it does not alter the key findings here (but leads to unwieldy expressions). Keeping conditions constant at a point where stomata will be open then dramatically overestimates total assimilation. However, the interest here is in the relation between climate and plant traits rather than exactly quantifying net gain and net cost of carbon investment.

As with all models, approximations and simplifications are required. One simplification is ignoring the role of plant water storage (PWS). The PWS is usually assumed to have negligible effects in other stomatal optimization models due to the relatively small water storage capacity of most C_3 and C_4 plants (Wang *et al.*, 2020). PWS introduces a time lag between soil and leaf water potential on diurnal time scales, but does not

fundamentally change any relations we are concerned with in the long term (Huang *et al.*, 2017).

The results here suggest that optimality imposes a constraint on the relation between climate and various plant traits, as well as between different traits related to resilience within a plant. Specifically, the first result here shows that xylem resilience to embolism should increase with drier average climates. The second result suggests that plants should invest such that their xylem (ψ_{50K}) are about twice as resilient to water stress as their photosynthetic apparatus (ψ_{50L}). This finding is also congruent with the hydraulic segmentation hypothesis as leaves are 'cheaper' to replace than xylem. Finally, it was shown that the coordination of many other plant traits, including carboxylation capacity and electron flux resilience to ψ_l can be shown to be optimal using similar methods.

The result that optimal $\psi_{50K} \approx 2\psi_{50L}$ is nonobvious. Physiologically, a 2 : 1 relation can be explained because of the push and pull between limitations on photosynthesis. A greater xylem resilience (more negative ψ_{50K}) allows for a greater flux of water through the plant and thus a higher stomatal conductance can be maintained. On the other hand, a greater NSL resilience (more negative ψ_{50L}) means photosynthesis is not limited. In other words, ψ_{50K} has a positively increasing relation with potential carbon assimilation, whereas the gain from ψ_{50L} plateaus once it is not limiting. Thus, investing in ψ_{50K} would yield a greater benefit than ψ_{50L}, but the two are constrained to be near each other so that neither one becomes limiting to carbon input and the water supply needed to maintain this input. Mathematically, the constraint appears through the multiplication of the logistic functions in Eqns 6 and S1.5 (in Methods S1). When changing the parameters of the system, the slope of the optimal $\psi_{50K} - \psi_{50L}$ line deviates slightly from 2 but remains within *c.* ±20%. Furthermore, different, valid methods for modeling plant processes could also lead to variations in this result, and further theoretical and empirical work is recommended to explore their outcome.

Conclusion

While optimality principles have long been used to describe plant function (Bloom *et al.*, 1985), a new economics based approach is applied to predict vulnerability curves from optimality arguments, thus effectively coupling short- and long-term optimization. The outcome of this application demonstrates mathematically the principle of co-limitation (Bloom *et al.*, 1985) and why resistance should increase with climate aridity. Trait coordination through long-term optimality here predicts a roughly 2 : 1 relation between the water potential at which xylem conductance is halved, ψ_{50K}, and the water potential at which photosynthetic capacity is limited by nonstomatal limitations, ψ_{50L}. This agrees with the limited data available. Full verification must wait future experiments where both short- and long-term water-carbon relations and associated traits are measured.

Nonstomatal limitations are an underinvestigated but increasingly recognized component for exploring plant function. The results here suggest that it may be possible to extrapolate from knowledge of the more widely available ψ_{50K} to determine ψ_{50L}. Needless to say, verification through empirical studies remains necessary before definitive conclusions can be drawn. Optimization theories often seek to isolate one aspect of plant function and assume other aspects are static. By integrating short- and long-term traits we have demonstrated a new method to explore optimizations of multiple traits across time scales. Going forward, the framework developed can be applied to other plant traits and processes, including the role of vulnerability curve slope on isohydricity and plant responses to salinity over different time scales.

Acknowledgements

AM was supported by High Meadows Environmental Institute. AP gratefully acknowledges support from the Carbon Mitigation Initiative at Princeton. GK acknowledges support from the U.S. National Science Foundation (NSF-AGS-2028633) and the Department of Energy (DESC0022072).

Competing interests

None declared.

Author contributions

All authors devised and planned the development of the research. AM developed the model and wrote the first draft, under the supervision of AP. AP and GK revised and contributed sections. All authors contributed to the final edits and revisions.

ORCID

Amilcare Porporato https://orcid.org/0000-0001-9378-207X

Data availability

Data in Fig. 3 from Manzoni (2014). Data in Fig. 4 from Zhou *et al.* (2014).

References

Ball JT, Woodrow IE, Berry JA. 1987. A model predicting stomatal conductance and its contribution to the control of photosynthesis under different environmental conditions. In: Biggins J, ed. *Progress in photosynthesis research.* Dordrecht, the Netherlands: Springer Netherlands, 221–224.

Binger B, Hoffman E. 1998. *Microeconomics with calculus, 2nd edn.* London, UK: AddisonWesley Educational.

Bloom AJ, Chapin FS, Mooney HA. 1985. Resource limitation in plants – an economic analogy. *Annual Review of Ecology and Systematics* **16**: 363–392.

Bonner J. 1959. Water transport: this classical problem in plant physiology is becoming increasingly amenable to mathematical analysis. *Science* **129**: 447–450.

Brodribb TJ, McAdam SA, Carins Murphy MR. 2017. Xylem and stomata, coordinated through time and space: functional linkages between xylem and stomata. *Plant, Cell & Environment* **40**: 872–880.

Buckley TN. 2017. Modeling stomatal conductance. *Plant Physiology* **174**: 572–582.

Buckley TN, Sack L, Farquhar GD. 2017. Optimal plant water economy. *Plant, Cell & Environment* **40**: 881–896.

Chen J-L, Reynolds JF, Harley PC, Tenhunen JD. 1993. Coordination theory of leaf nitrogen distribution in a canopy. *Oecologia* **93**: 63–69.

Choat B, Sack L, Michele Holbrook N. 2007. Diversity of hydraulic traits in nine *Cordia* species growing in tropical forests with contrasting precipitation. *New Phytologist* **175**: 686–698.

Daly E, Porporato A, Rodriguez-Iturbe I. 2004. Coupled dynamics of photosynthesis, transpiration, and soil water balance. Part I: upscaling from hourly to daily level. *Journal of Hydrometeorology* **5**: 546–558.

Damour G, Simonneau T, Cochard H, Urban L. 2010. An overview of models of stomatal conductance at the leaf level: models of stomatal conductance. *Plant, Cell & Environment* **33**: 1419–1438.

Dewar R, Holttä T, Salmon Y. 2022. Exploring optimal stomatal control under alternative hypotheses for the regulation of plant sources and sinks. *New Phytologist* **233**: 639–654.

Dewar R, Mauranen A, Mäkelä A, Hölttä T, Medlyn B, Vesala T. 2018. New insights into the covariation of stomatal, mesophyll and hydraulic conductances from optimization models incorporating nonstomatal limitations to photosynthesis. *New Phytologist* **217**: 571–585.

Diaz-Espejo A, Hernandez-Santana V. 2017. The phloem–xylem consortium: until death do them part. *Tree Physiology* **37**: 847–850.

Ehleringer JR, Cowan IR. 1986. Economics of carbon fixation. In: Givnish TJ, ed. *On the economy of plant form and function*. Cambridge, UK: Cambridge University Press, 133–170.

Farquhar GD, von Caemmerer S, Berry JA. 1980. A biochemical model of photosynthetic CO_2 assimilation in leaves of C_3 species. *Planta* **149**: 78–90.

Flexas J, Carriquí M, Nadal M. 2018. Gas exchange and hydraulics during drought in crops: who drives whom? *Journal of Experimental Botany* **69**: 3791–3795.

Flexas J, Ribas-Carbó M, Diaz-Espejo A, Galmés J, Medrano H. 2008. Mesophyll conductance to CO_2: current knowledge and future prospects. *Plant, Cell & Environment* **31**: 602–621.

Hacke UG, Sperry JS, Pittermann J. 2004. Analysis of circular bordered pit function II. Gymnosperm tracheids with torus-margo pit membranes. *American Journal of Botany* **91**: 386–400.

Holttä T, Lintunen A, Chan T, Mäkelä A, Nikinmaa E. 2017. A steady-state stomatal model of balanced leaf gas exchange, hydraulics and maximal source–sink flux. *Tree Physiology* **37**: 851–868.

Huang C-W, Domec J-C, Ward EJ, Duman T, Manoli G, Parolari AJ, Katul GG. 2017. The effect of plant water storage on water fluxes within the coupled soil–plant system. *New Phytologist* **213**: 1093–1106.

Jensen KH, Berg-Sørensen K, Bruus H, Holbrook NM, Liesche J, Schulz A, Zwieniecki MA, Bohr T. 2016. Sap flow and sugar transport in plants. *Reviews of Modern Physics* **88**: 035007.

Johnson DM. 2014. An assessment of pre- and within-season remotely sensed variables for forecasting corn and soybean yields in the United States. *Remote Sensing of Environment* **141**: 116–128.

Johnson DM, Katul G, Domec J-C. 2022. Catastrophic hydraulic failure and tipping points in plants. *Plant, Cell & Environment* **45**: 2231–2266.

Kannenberg SA, Guo JS, Novick KA, Anderegg WRL, Feng X, Kennedy D, Konings AG, Martínez-Vilalta J, Matheny AM. 2022. Opportunities, challenges and pitfalls in characterizing plant water-use strategies. *Functional Ecology* **36**: 24–37.

Katul G, Oren R, Manzoni S, Higgins C, Parlange MB. 2012. Evapotranspiration: a process driving mass transport and energy exchange in the soil-plant-atmosphere-climate system. *Reviews of Geophysics* **50**: 1–25.

Konrad W, Katul G, Roth-Nebelsick A, Jensen KH. 2019. Xylem functioning, dysfunction and repair: a physical perspective and implications for phloem transport. *Tree Physiology* **39**: 243–261.

Lai C-T, Katul G, Oren R, Ellsworth D, Schäfer K. 2000. Modeling CO_2 and water vapor turbulent flux distributions within a forest canopy. *Journal of Geophysical Research: Atmospheres* **105**: 26333–26351.

Lens F, Gleason SM, Bortolami G, Brodersen C, Delzon S, Jansen S. 2022. Functional xylem characteristics associated with drought-induced embolism in angiosperms. *New Phytologist* **236**: 2019–2036.

Leuning R. 1995. A critical appraisal of a combined stomatal-photosynthesis model for C_3 plants. *Plant, Cell & Environment* **18**: 339–355.

Leuning R. 1997. Scaling to a common temperature improves the correlation between the photosynthesis parameters J_{max} and V_{cmax}. *Journal of Experimental Botany* **48**: 345–347.

Li S, Hamani AKM, Zhang Y, Liang Y, Gao Y, Duan A. 2021. Coordination of leaf hydraulic, anatomical, and economical traits in tomato seedlings acclimation to long-term drought. *BMC Plant Biology* **21**: 536.

Manoli G, Huang C-W, Bonetti S, Domec J-C, Marani M, Katul G. 2017. Competition for light and water in a coupled soil-plant system. *Advances in Water Resources* **108**: 216–230.

Manzoni S. 2014. Integrating plant hydraulics and gas exchange along the drought-response trait spectrum. *Tree Physiology* **34**: 1031–1034.

Manzoni S, Katul G, Porporato A. 2014. A dynamical system perspective on plant hydraulic failure. *Water Resources Research* **50**: 5170–5183.

Manzoni S, Vico G, Katul G, Fay PA, Polley W, Palmroth S, Porporato A. 2011. Optimizing stomatal conductance for maximum carbon gain under water stress: a meta-analysis across plant functional types and climates. *Functional Ecology* **25**: 456–467.

Manzoni S, Vico G, Katul G, Palmroth S, Jackson RB, Porporato A. 2013a. Hydraulic limits on maximum plant transpiration and the emergence of the safety–efficiency trade-off. *New Phytologist* **198**: 169–178.

Manzoni S, Vico G, Porporato A, Katul G. 2013b. Biological constraints on water transport in the soil–plant–atmosphere system. *Advances in Water Resources* **51**: 292–304.

Mencuccini M. 2003. The ecological significance of long-distance water transport: short-term regulation, long-term acclimation and the hydraulic costs of stature across plant life forms: ecological significance of xylem water transport. *Plant, Cell & Environment* **26**: 163–182.

Mencuccini M, Minunno F, Salmon Y, Martínez-Vilalta J, Hölttä T. 2015. Coordination of physiological traits involved in drought-induced mortality of woody plants. *New Phytologist* **208**: 396–409.

Mrad A, Domec J-C, Huang C-W, Lens F, Katul G. 2018. A network model links wood anatomy to xylem tissue hydraulic behaviour and vulnerability to cavitation. *Plant, Cell & Environment* **41**: 2718–2730.

Mrad A, Sevanto S, Domec J-C, Liu Y, Nakad M, Katul G. 2019. A dynamic optimality principle for water use strategies explains isohydric to anisohydric plant responses to drought. *Frontiers in Forests and Global Change* **2**: 49.

Nakad M, Sevanto S, Domec JC, Katul G. 2023. Linking the water and carbon economies of plants in a drying and warming climate. *Current Forestry Reports* **9**: 383–400.

Nakad M, Witelski T, Domec JC, Sevanto S, Katul G. 2021. Taylor dispersion in osmotically driven laminar flows in phloem. *Journal of Fluid Mechanics* **913**: A44.

Nikinmaa E, Hölttä T, Hari P, Kolari P, Mäkelä A, Sevanto S, Vesala T. 2013. Assimilate transport in phloem sets conditions for leaf gas exchange. *Plant, Cell & Environment* **36**: 655–669.

Novick KA, Katul GG, McCarthy HR, Oren R. 2012. Increased resin flow in mature pine trees growing under elevated CO_2 and moderate soil fertility. *Tree Physiology* **32**: 752–763.

Porporato A, Yin J. 2022. *Ecohydrology*. Cambridge, UK: Cambridge University Press.

Potkay A, Feng X. 2022. Do stomata optimize turgor-driven growth? A new framework for integrating stomata response with whole-plant hydraulics and carbon balance. *New Phytologist* **238**: 506–528.

Qiu R, Katul GG. 2020. Maximizing leaf carbon gain in varying saline conditions: an optimization model with dynamic mesophyll conductance. *The Plant Journal* **101**: 543–554.

Reich PB. 2014. The world-wide 'fast-slow' plant economics spectrum: a traits manifesto. *Journal of Ecology* **102**: 275–301.

Roff DA, Fairbairn DJ. 2007. The evolution of trade-offs: where are we? *Journal of Evolutionary Biology* **20**: 433–447.

Salvi AM, Smith DD, Adams MA, McCulloh KA, Givnish TJ. 2021. Mesophyll photosynthetic sensitivity to leaf water potential in *Eucalyptus*: a new dimension of plant adaptation to native moisture supply. *New Phytologist* **230**: 1844–1855.

Sevanto S. 2014. Phloem transport and drought. *Journal of Experimental Botany* **65**: 1751–1759.

Sperry JS, Hacke UG. 2004. Analysis of circular bordered pit function I. Angiosperm vessels with homogenous pit membranes. *American Journal of Botany* **91**: 369–385.

Sperry JS, Venturas MD, Anderegg WRL, Mencuccini M, Mackay DS, Wang Y, Love DM. 2017. Predicting stomatal responses to the environment from the optimization of photosynthetic gain and hydraulic cost: a stomatal optimization model. *Plant, Cell & Environment* **40**: 816–830.

Sperry JS, Wang Y, Wolfe BT, Mackay DS, Anderegg WRL, McDowell NG, Pockman WT. 2016. Pragmatic hydraulic theory predicts stomatal responses to climatic water deficits. *New Phytologist* **212**: 577–589.

Thompson MV, Holbrook NM. 2003. Scaling phloem transport: water potential equilibrium and osmoregulatory flow. *Plant, Cell & Environment* **26**: 1561–1577.

Tuzet A, Perrier A, Leuning R. 2003. A coupled model of stomatal conductance, photosynthesis and transpiration. *Plant, Cell & Environment* **26**: 1097–1116.

Tyree MT, Sperry JS. 1988. Do woody plants operate near the point of catastrophic xylem dysfunction caused by dynamic water stress? Answers from a model. *Plant Physiology* **88**: 574–580.

Van den Honert TH. 1948. Water transport in plants as a catenary process. *Discussions of the Faraday Society* **3**: 146–153.

Vico G, Manzoni S, Palmroth S, Katul G. 2011. Effects of stomatal delays on the economics of leaf gas exchange under intermittent light regimes. *New Phytologist* **192**: 640–652.

Vico G, Porporato A. 2008. Modelling C_3 and C_4 photosynthesis under waterstressed conditions. *Plant and Soil* **313**: 187–203.

Volpe V, Manzoni S, Marani M, Katul G. 2011. Leaf conductance and carbon gain under salt-stressed conditions. *Journal of Geophysical Research: Biogeosciences* **116**: 1–12.

Wang Y, Sperry JS, Anderegg WRL, Venturas MD, Trugman AT. 2020. A theoretical and empirical assessment of stomatal optimization modeling. *New Phytologist* **227**: 311–325.

Wolf A, Anderegg WRL, Pacala SW. 2016. Optimal stomatal behavior with competition for water and risk of hydraulic impairment. *Proceedings of the National Academy of Sciences, USA* **113**: E7222–E7230.

Xu H, Wang H, Prentice IC, Harrison SP, Wright IJ. 2021. Coordination of plant hydraulic and photosynthetic traits: confronting optimality theory with field measurements. *New Phytologist* **232**: 1286–1296.

Zhou S, Duursma RA, Medlyn BE, Kelly JWG, Prentice IC. 2013. How should we model plant responses to drought? An analysis of stomatal and non-stomatal responses to water stress. *Agricultural and Forest Meteorology* **182–183**: 204–214.

Zhou S, Medlyn B, Sabaté S, Sperlich D, Prentice IC, Whitehead D. 2014. Short-term water stress impacts on stomatal, mesophyll and biochemical limitations to photosynthesis differ consistently among tree species from contrasting climates. *Tree Physiology* **34**: 1035–1046.

Zimmermann MH. 2013. *Xylem structure and the ascent of sap*. Berlin, Germany: Springer Science & Business Media.

Supporting Information

Additional Supporting Information may be found online in the Supporting Information section at the end of the article.

Methods S1 Description of the photosynthesis model used.

Please note: Wiley is not responsible for the content or functionality of any Supporting Information supplied by the authors. Any queries (other than missing material) should be directed to the *New Phytologist* Central Office.